

Two-loop amplitudes for $qg \rightarrow Hq$ and $q\bar{q} \rightarrow Hg$ mediated by a nearly massless quark

Kirill Melnikov^{a, 1}, Lorenzo Tancredi^{a, 2}, Christopher Wever^{a,b, 3}

^a *Institute for Theoretical Particle Physics, KIT, 76128 Karlsruhe, Germany*

^b *Institut für Kernphysik, KIT, 76344 Eggenstein-Leopoldshafen, Germany*

Abstract

We compute the two-loop QCD corrections to $qg \rightarrow Hq$ and $q\bar{q} \rightarrow Hg$ amplitudes mediated by loops of nearly massless quarks. These amplitudes provide the last missing ingredient required to compute the NLO QCD corrections to the top-bottom interference contribution to the Higgs boson transverse momentum distribution at hadron colliders.

Key words: QCD, Higgs physics, multi-loop computations, asymptotic expansion

¹e-mail: kirill.melnikov@kit.edu

²e-mail: lorenzo.tancredi@kit.edu

³e-mail: christopher.wever@kit.edu

1 Introduction

A Standard Model (SM)-like Higgs boson was discovered at the LHC in 2012. An important step in “fingerprinting” this particle is the precise determination of its couplings to quarks, leptons and gauge bosons. Indeed, couplings of the SM Higgs boson to other particles should be related to particle masses and the exact relation between these particle masses and their couplings to the Higgs can be derived with an astounding precision in the SM. Results from the Run I of the LHC seem to indicate that the Higgs couplings to SM fermions and vector bosons are in agreement with the expectations, within current statistical and systematic errors.

The precision of the Higgs couplings measurements is expected to increase as more data from Run II is analyzed; by the end of the high-luminosity phase of the LHC it is conceivable that $\mathcal{O}(\text{few})$ -percent measurements of the Higgs couplings will become available. Motivated by this, theoretical predictions for Higgs boson production cross sections at the LHC and for Higgs boson decays were extended to very high orders in perturbative QCD and the SM, resulting in high precision for observables relevant for Higgs phenomenology. The recent highlight of this activity is the calculation of the inclusive cross section of the dominant $gg \rightarrow H$ production process through N³LO QCD in the infinite top mass limit [1]. However, thanks to increased energy and statistics of the LHC Run II, it is interesting to refine an understanding of more exclusive processes, for example production of the Higgs boson in association with a jet. In the $m_t \rightarrow \infty$ approximation, the NNLO QCD corrections to $pp \rightarrow H + j$ and to the Higgs transverse momentum were computed in Refs. [2–5].

While the above computations provide a clear milestone for applications of perturbative QCD to Higgs physics at hadron colliders, there are good reasons to go beyond the $m_t \rightarrow \infty$ approximation in theoretical predictions for $H + j$ and the Higgs p_\perp spectrum. Indeed, by measuring the Higgs transverse momentum distribution at high p_\perp , one can probe couplings of the Higgs boson to hypothetical top partners and constrain models beyond the SM [6]. A particular valuable is the kinematic region where the Higgs boson is produced with a large transverse momentum [7–10].¹ A comparison with future high- p_\perp experimental analysis will require accurate theoretical predictions for exclusive Higgs production in association with one or more jets.

It is also interesting to consider low and moderate transverse momenta of the produced Higgs bosons since this is where the bulk of the events is. At values of the Higgs transverse momentum $p_\perp < m_t$, the top quark loop is, essentially, point-like but the bottom quark loop is not. Naively, the bottom quark loop is expected to be suppressed by a factor of $y_b m_b/m_h \sim m_b^2/m_h^2 \sim 10^{-3}$ relative to the top quark loop but, as it turns out, the reality is more complex. Indeed, it is known that the bottom quark loop is enhanced by a logarithm of the ratio of the Higgs boson mass to the b -quark mass, $\log^2(m_h^2/m_b^2) \sim \text{few} \times 10$, so that the bottom loop contribution is estimated to change the top loop result by five to ten percent.

We note that the structure of logarithms is actually more complicated for observables that are less exclusive than the inclusive Higgs production cross section. For example, double logarithms of the form $\log^2(p_\perp^2/m_b^2)$ appear in Higgs transverse momentum distribution for $p_\perp \gg m_b$ leading to enhanced, kinematics-dependent corrections [12–15]. Existing numerical estimates point towards a few percent effects that are caused by top-bottom p_\perp -dependent

¹See [11] for further references.

interference contributions. Therefore, since the QCD corrections to Higgs boson production in gluon fusion are known to be large and since a few percent precision on Higgs production cross sections is a long-term goal of the LHC program, it is important to compute the NLO QCD corrections to the bottom loop.

Another reason to consider NLO QCD corrections to bottom-quark-mediated contributions to Higgs boson production is more theoretical in nature. Indeed, as we already mentioned, new double logarithmic terms appear in the perturbative expansion but these logarithms are not very well understood so that, for example, their resummation can not be currently performed.² To this end, explicit NLO calculations of the relevant scattering amplitude provide an important “data point” for future efforts to understand and, perhaps, resum quark-mass dependent logarithmic corrections in Higgs boson production.

We have laid the groundwork for such a NLO computation in Ref. [18] by calculating the $gg \rightarrow Hg$ amplitudes mediated by a bottom quark, in the limit $m_b \rightarrow 0$.³ In this paper we compute the $m_b \rightarrow 0$ limit of the quark-gluon amplitude, relevant for the remaining partonic channels $q\bar{q} \rightarrow Hg$ and $qg \rightarrow Hq$.⁴ The calculation of these two-loop amplitudes retaining exact mass dependence remains an outstanding task. A first promising step in this direction has been recently taken with the calculation of the relevant planar master integrals [20]. The results that we present in this paper complement those of Ref. [18] and, together, provide all two-loop amplitudes required for the computation of NLO QCD corrections to top-bottom interference effects in the production of the Higgs boson in association with a jet, and in the Higgs boson transverse momentum distribution.

The paper is organized as follows. We explain the notation and discuss the Lorentz structure of the relevant amplitudes in Section 2. In Sections 3 and 4 we review the computation of the form factors and describe their renormalization. We present the results for the helicity amplitudes in Section 5. For reasons of convenience, the amplitudes are first computed in the decay kinematics, i.e. for the process $H \rightarrow q\bar{q}g$. Their analytic continuation to the kinematic regions relevant for Higgs boson production is described in Section 6. The limit of the helicity amplitudes for the physical scattering process $qg \rightarrow Hq$, where the initial and final state quark are collinear, is considered in Section 7. We conclude in Section 8. Analytic results for the amplitudes in different kinematic regions are attached as ancillary files to the arXiv submission of this paper.

2 Lorentz structure of the scattering amplitude

We consider the process

$$H(p_4) \rightarrow q(p_1) + \bar{q}(p_2) + g(p_3), \quad (2.1)$$

mediated by a bottom quark with the mass m_b . We introduce the usual Mandelstam variables

$$s = (p_1 + p_2)^2, \quad t = (p_1 + p_3)^2, \quad u = (p_2 + p_3)^2, \quad s + t + u = m_h^2, \quad (2.2)$$

²Such corrections in the abelian limit and in the high-energy limit were studied to all orders in α_s in Refs. [16, 17].

³A similar approach has been used to study top-bottom interference effects in single Higgs production in Ref. [19].

⁴We note that we do not consider amplitudes where bottom quark appears as an external particle.

where m_h is the Higgs boson mass. We consider the process in the kinematic limit where the bottom mass is the smallest scale in the problem; this implies that $m_b^2 \ll s \sim t \sim u \sim m_h^2$. Following Ref. [18], we introduce the massless ratios

$$x = \frac{s}{m_h^2}, \quad y = \frac{t}{m_h^2}, \quad z = \frac{u}{m_h^2}, \quad \kappa = -\frac{m_b^2}{m_h^2}, \quad (2.3)$$

and consider the amplitude in decay kinematics. This implies

$$0 < y < 1, \quad 0 < z < 1, \quad 0 < x = 1 - y - z < 1, \quad \kappa > 0, \quad m_h^2 > 0. \quad (2.4)$$

With these choices, the only source of imaginary parts in contributing Feynman integrals is the positive value of the Higgs mass, that can be isolated as an overall prefactor $(-m_h^2 - i0)^{-\epsilon}$ per loop.

We define the partonic scattering amplitude as follows⁵

$$\mathcal{A}(p_1^j, p_2^k, p_3^a) = i T_{jk}^a \epsilon_3^\mu(p_3) \bar{u}(p_1) \mathcal{A}_\mu(s, t, u, m_b) v(p_2), \quad (2.5)$$

where j, k are the color indices of the quark and the antiquark, respectively, and a is the color index of the gluon. The amplitude $\mathcal{A}(p_1^j, p_2^k, p_3^a)$ should be Lorentz-invariant and transversal

$$p_3^\mu \bar{u}(p_1) \mathcal{A}_\mu(s, t, u, m_b) v(p_2) = 0. \quad (2.6)$$

The most general ansatz for \mathcal{A}_μ consistent with these conditions and parity conservation involves two form factors

$$\mathcal{A}^\mu = F_1 (\not{p}_3 p_2^\mu - p_2 \cdot p_3 \gamma^\mu) + F_2 (\not{p}_3 p_1^\mu - p_1 \cdot p_3 \gamma^\mu) = F_1 \tau_1^\mu + F_2 \tau_2^\mu. \quad (2.7)$$

We note that the two tensorial structures in Eq.(2.7) satisfy the transversality condition Eq.(2.6) separately. The form factors in Eq.(2.7) are Lorentz-scalar functions of the Mandelstam invariants $F_j = F_j(s, t, u, m_b)$.

The unrenormalized form factors F_j can be expanded in the strong coupling constant. We write

$$F_j^{\text{un}}(s, t, u, m_b) = \sqrt{\frac{\alpha_0^3}{\pi}} \left[F_j^{(1),\text{un}} + \left(\frac{\alpha_0}{2\pi}\right) F_j^{(2),\text{un}} + \mathcal{O}(\alpha_0^2) \right], \quad j = 1, 2, \quad (2.8)$$

where α_0 is the bare QCD coupling constants. The form factors $F_{1,2}^{(1)}$ are known, including the full dependence on the quark mass [21,22]. Our goal is to compute the NLO QCD contributions to the two form factors in $m_b \rightarrow 0$ limit.

3 Computation of the form factors

To compute the two form factors in Eq.(2.8), we proceed as described in Ref. [18], where $H \rightarrow ggg$ amplitudes were studied. The Feynman diagrams that contribute to the process Eq.(2.1) are produced with QGRAF [23] and independently with FeynArts [24]. Allowing for

⁵We only consider massless quarks in the initial and final states.

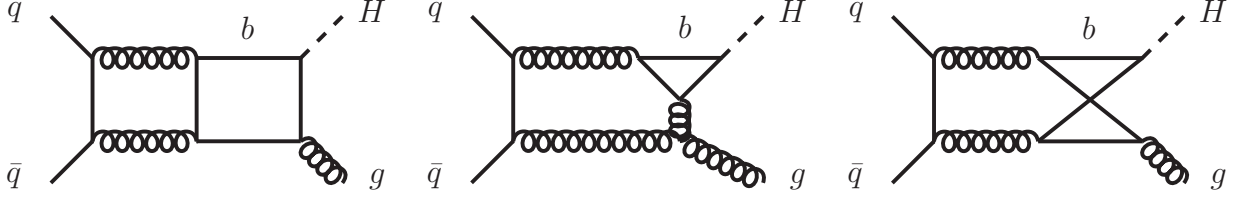


Figure 1: Examples of two-loop Feynman diagrams that contribute to the process $H \rightarrow q\bar{q}g$.

massless external quarks and both massive and massless internal quarks, we find two diagrams at one loop and 49 at two loops; examples are shown in Figure 1.

The two form factors are extracted by applying projection operators to individual Feynman diagrams. We use the same notation as in Ref. [25] and define

$$T_1^\mu = \bar{u}(p_1)\tau_1^\mu v(p_2), \quad T_2^\mu = \bar{u}(p_1)\tau_2^\mu v(p_2). \quad (3.1)$$

In terms of $T_{1,2}^\mu$, the projection operators read

$$\mathcal{P}^\mu(F_1) = \frac{1}{2(d-3)st} \left[\frac{(d-2)}{t} (T_1^\mu)^\dagger - \frac{(d-4)}{u} (T_2^\mu)^\dagger \right], \quad (3.2)$$

$$\mathcal{P}^\mu(F_2) = \frac{1}{2(d-3)su} \left[\frac{(d-2)}{u} (T_2^\mu)^\dagger - \frac{(d-4)}{t} (T_1^\mu)^\dagger \right]. \quad (3.3)$$

Their action on the amplitude is described by the following formula

$$F_i(s, t, u, m_b) = \sum_{pol} \mathcal{P}^\mu(F_i) (\epsilon_{3,\mu}(p_3))^* \epsilon_3^\nu(p_3) \mathcal{A}_\nu(s, t, u, m_b), \quad (3.4)$$

where sums over quark, antiquark and gluon polarizations need to be computed. These polarization sums are calculated with the help of standard formulas

$$\sum_{pol} u(p_1)\bar{u}(p_1) = \not{p}_1, \quad \sum_{pol} v(p_2)\bar{v}(p_2) = \not{p}_2, \quad (3.5)$$

$$\sum_{pol} (\epsilon_3^\mu(p_3))^* \epsilon_3^\nu(p_3) = -g^{\mu\nu}. \quad (3.6)$$

We note that it is allowed to use unphysical result for the sum over gluon polarizations as in Eq.(3.6) since the tensor structures $T_{1,2}^\mu$ satisfy the transversality condition independently.

The algebraic manipulations required to apply the projection operators to the amplitudes, perform the polarization sums and extract the form factors have been carried out independently using both FORM [26] and FormCalc [27]. After performing the Lorentz algebra, the form factors are expressed as linear combinations of scalar integrals

$$\mathcal{I}_{\text{top}}(a_1, a_2, \dots, a_8, a_9) = \int \frac{\mathfrak{D}^d k \mathfrak{D}^d l}{[1]^{a_1} [2]^{a_2} [3]^{a_3} [4]^{a_4} [5]^{a_5} [6]^{a_6} [7]^{a_7} [8]^{a_8} [9]^{a_9}}, \quad (3.7)$$

with the integration measure defined as

$$\mathfrak{D}^d k = (-m_h^2)^{(4-d)/2} \frac{(4\pi)^{d/2}}{i\Gamma(1+\epsilon)} \int \frac{d^d k}{(2\pi)^d}. \quad (3.8)$$

Prop.	Topology PL1	Topology PL2	Topology NPL
[1]	k^2	$k^2 - m_b^2$	$k^2 - m_b^2$
[2]	$(k - p_1)^2$	$(k - p_1)^2 - m_b^2$	$(k + p_1)^2 - m_b^2$
[3]	$(k - p_1 - p_2)^2$	$(k - p_1 - p_2)^2 - m_b^2$	$(k - p_2 - p_3)^2 - m_b^2$
[4]	$(k - p_1 - p_2 - p_3)^2$	$(k - p_1 - p_2 - p_3)^2 - m_b^2$	$l^2 - m_b^2$
[5]	$l^2 - m_b^2$	$l^2 - m_b^2$	$(l + p_1)^2 - m_b^2$
[6]	$(l - p_1)^2 - m_b^2$	$(l - p_1)^2 - m_b^2$	$(l - p_3)^2 - m_b^2$
[7]	$(l - p_1 - p_2)^2 - m_b^2$	$(l - p_1 - p_2)^2 - m_b^2$	$(k - l)^2$
[8]	$(l - p_1 - p_2 - p_3)^2 - m_b^2$	$(l - p_1 - p_2 - p_3)^2 - m_b^2$	$(k - l - p_2)^2$
[9]	$(k - l)^2 - m_b^2$	$(k - l)^2$	$(k - l - p_2 - p_3)^2$

Table 1: Feynman propagators of the three integral families, see Eq.(3.7).

As discussed in Ref. [18], the scalar integrals shown in Eq.(3.7) can be organized into three integral families. For convenience we provide their definitions in Table 1.

Similarly to the case of the $H \rightarrow ggg$ amplitude, all scalar integrals that are required for the $H \rightarrow q\bar{q}g$ amplitude can be reduced to master integrals (MIs) using integration by parts identities [28, 29]. However, in the qg case, the most complicated non-planar sector does not contribute to the amplitude and the reduction can be performed entirely using the public codes FIRE5 [30, 31] and Reduze2 [32–35]. All the relevant MIs have been computed in Ref. [18] with the method of differential equations, as an expansion in κ . As a result we obtain analytic expressions for the form factors to leading order in κ and up to order ϵ^2 and ϵ^0 for their one- and two-loop contributions, respectively. It is well known, that the expansion for small values of κ is non-analytic and the one- and two-loop form factors develop logarithmic singularities $\propto \log(\kappa)$ as $\kappa \rightarrow 0$. Written in terms of m_h^2 and the dimensionless variables y, z, κ , the unrenormalized form factors have the following expansion

$$\lim_{m_b \rightarrow 0} F_j^{(1),\text{un}}(y, z, \kappa, m_h^2) = \frac{m_b^2}{v} \frac{1}{m_h^4} \sum_{n=0}^2 \epsilon^n \sum_{a=0}^4 f_{a,j}^{(1l,n)}(y, z) \log^a \kappa, \quad (3.9)$$

$$\lim_{m_b \rightarrow 0} F_j^{(2),\text{un}}(y, z, \kappa, m_h^2) = \frac{m_b^2}{v} \frac{1}{m_h^4} \sum_{n=-2}^0 \epsilon^n \sum_{a=0}^4 f_{a,j}^{(2l,n)}(y, z) \log^a \kappa, \quad (3.10)$$

where v is the Higgs vacuum expectation value. One of the two powers of the bottom quark mass m_b shown in Eqs.(3.9, 3.10) has its origin in the Yukawa coupling $b\bar{b}H$ and the other in the helicity flip on one of the bottom quark lines required to enable the ggH coupling through the bottom quark loop. The coefficients in this expansion $f_{a,j}^{(1l,n)}(y, z)$ and $f_{a,j}^{(2l,n)}(y, z)$ can all be expressed in terms of a subset of Goncharov polylogarithms known as 2dHPLs. They were defined in Ref. [36]. We refer to Ref. [18] for additional details on how to efficiently compute MIs in the limit of vanishing quark masses, $\kappa \rightarrow 0$.

4 Ultraviolet renormalization and extraction of infrared singularities

The bare form factors are regularized dimensionally and contain poles in $\epsilon = (4 - d)/2$. These poles originate from ultraviolet (UV) and infrared (IR) divergences of loop integrals that contribute to the scattering amplitude. These divergences are either removed by UV renormalization or cancel against real emission contributions when physical cross sections are calculated. The relevant information is contained in suitably-defined finite parts of the amplitudes whose computation we now describe.

To render the amplitudes finite, we first subtract the UV poles and write the UV renormalized form factors as

$$F_j^{\text{UV}}(s, t, u, m_b) = \sqrt{\frac{\alpha_s^3}{\pi S_\epsilon^3}} \left[F_j^{(1),\text{UV}} + \left(\frac{\alpha_s}{2\pi}\right) F_j^{(2),\text{UV}} + \mathcal{O}(\alpha_s^3) \right]. \quad (4.1)$$

Renormalized form factors are obtained from the bare ones F_j^{un} in Eq.(2.8) by expressing bare parameters in terms of their renormalized counterparts and including the wave-function renormalization factor for each external gluon. The massless quark contributions to the coupling constant are renormalized in the $\overline{\text{MS}}$ -scheme, while the bottom-quark contribution is renormalized at zero-momentum transfer. Choosing a “physical” renormalization scheme for the bottom quark mass is more tricky, see discussion in Ref. [18]. For simplicity, we renormalize the bottom mass in the on-shell scheme. Relations between bare and renormalized parameters are described by the following equations

$$\alpha_0 \mu_0^{2\epsilon} S_\epsilon = \alpha_s \mu_R^{2\epsilon} \left[1 - \frac{1}{\epsilon} (\beta_0 + \delta_w) \left(\frac{\alpha_s}{2\pi}\right) + \mathcal{O}(\alpha_s^2) \right], \quad (4.2)$$

$$m_{b,0} = m_b \left[1 + \left(\frac{\alpha_s}{2\pi}\right) \delta_m + \mathcal{O}(\alpha_s^2) \right], \quad (4.3)$$

where $S_\epsilon = (4\pi)^\epsilon e^{-\epsilon\gamma_E}$, $\gamma_E = 0.5772\dots$, $\beta_0 = 11/6 C_A - 2/3 T_R N_f$, $T_R = 1/2$. In addition, $C_A = N_c$ is the number of colors and N_f is the number of massless quark flavors. The renormalization constants read

$$\delta_w = -2/3 T_R (m_b^2/\mu_R^2)^{-\epsilon}, \quad \delta_m = C_F \left(\frac{m_b^2}{\mu_R^2}\right)^{-\epsilon} \left(-\frac{3}{2\epsilon} - 2 + \mathcal{O}(\epsilon)\right). \quad (4.4)$$

Gluon wave function renormalization is performed by multiplying the form factors with

$$Z_A^{1/2} = \left(1 + \left(\frac{\alpha_s}{2\pi}\right) \delta_w + \mathcal{O}(\alpha_s^2) \right)^{1/2} = 1 + \frac{1}{2} \left(\frac{\alpha_s}{2\pi}\right) \delta_w + \mathcal{O}(\alpha_s^2),$$

for each external gluon in the process. Putting everything together, we find that the UV-renormalized and bare form factors are related by

$$\begin{aligned} F_j^{(1),\text{UV}} &= F_j^{(1),\text{un}}, \\ F_j^{(2),\text{UV}} &= S_\epsilon^{-1} F_j^{(2),\text{un}} - \left(\frac{3\beta_0}{2\epsilon} + \frac{\delta_w}{\epsilon}\right) F_j^{(1),\text{un}} + m_b \frac{dF_j^{(1),\text{un}}}{dm_b} \delta_m. \end{aligned} \quad (4.5)$$

Even after UV renormalization, the form factors still contain $1/\epsilon$ divergences that reflect the infrared singularities of scattering amplitudes. These infrared singularities are universal [37]; this implies that infrared divergences of a two-loop QCD amplitude for a given process can be predicted in terms of Born and one-loop amplitudes for that process. Since the amplitude $0 \rightarrow H + q\bar{q} + g$ appears at one-loop, the infrared structure of the two-loop amplitude is that of next-to-leading order and, therefore, simple. We have [37]

$$F_j^{(1),\text{UV}} = F_j^{(1),\text{fin}}, \quad F_j^{(2),\text{UV}} = I_1(\epsilon)F_j^{(1),\text{UV}} + F_j^{(2),\text{fin}}, \quad (4.6)$$

where $F_{1,2}^{\text{fin}}$ are finite in the limit $\epsilon \rightarrow 0$. The operator $I_1(\epsilon)$ contains all infrared singularities; for a process with a quark, antiquark and a gluon it assumes the following form

$$I_1(\epsilon) = -\frac{e^{\epsilon\gamma}}{2\Gamma(1-\epsilon)} \left(C_A \left(\frac{1}{\epsilon^2} + \frac{3}{4\epsilon} + \frac{\beta_0}{2C_A\epsilon} \right) \left(\left(-\frac{t}{\mu_R^2} \right)^{-\epsilon} + \left(-\frac{u}{\mu_R^2} \right)^{-\epsilon} \right) - \frac{1}{C_A} \left(\frac{1}{\epsilon^2} + \frac{3}{2\epsilon} \right) \left(-\frac{s}{\mu_R^2} \right)^{-\epsilon} \right). \quad (4.7)$$

We note that because of the ϵ^2 poles that appear in the $I_1(\epsilon)$ operator, we require the one-loop amplitude to order ϵ^2 , as indicated in Eq.(3.9).

5 Helicity amplitudes

For phenomenological applications, it is useful to derive analytic expressions for the helicity amplitudes for the process $H \rightarrow q\bar{q}g$. We begin by expressing the helicity amplitudes through the form factors defined in Eq.(2.7). We use the spinor-helicity formalism (see e.g. [38]) and define positive and negative helicity spinors for massless external quarks as

$$\begin{aligned} u_+(p) &= v_-(p) = |p\rangle, & u_-(p) &= v_+(p) = |p], \\ \bar{u}_+(p) &= \bar{v}_-(p) = [p|, & \bar{u}_-(p) &= \bar{v}_+(p) = \langle p|. \end{aligned} \quad (5.1)$$

For the external gluon we define

$$\epsilon_{3,+}^\mu(p_3) = \frac{\langle q|\gamma^\mu|3\rangle}{\sqrt{2}\langle q3\rangle}, \quad \epsilon_{3,-}^\mu(p_3) = -\frac{[q|\gamma^\mu|3\rangle}{\sqrt{2}[q3]}, \quad (5.2)$$

where q is an arbitrary (light-like) reference vector.

We define the helicity amplitudes as

$$\mathcal{A}_{\lambda_1\lambda_2\lambda_3}(s, t, u, m_b) = \epsilon_{3,\lambda_3}^\mu(p_3)\bar{u}_{\lambda_1}(p_1)\mathcal{A}_\mu(s, t, u, m_b)v_{\lambda_2}(p_2). \quad (5.3)$$

Since QCD interactions do not change the helicities of massless fermions, the helicities of the quark and the antiquark in Eq.(5.3) are correlated. This implies that there are, in total, only four possible helicity configurations. Out of these four, only one is independent; the other

three can be obtained from it by charge and parity conjugation. We choose the amplitude \mathcal{A}_{-++} as an independent and obtain

$$\mathcal{A}_{-++}(s, t, u, m_b) = \frac{1}{\sqrt{2}} \frac{[23]^2}{[12] m_h^2} \Omega_{-++}(s, t, u, m_b), \quad (5.4)$$

where the helicity coefficient $\Omega_{-++}(s, t, u, m_b)$ is dimensionless. The amplitudes for the other helicity assignments can be obtained from \mathcal{A}_{-++} by complex conjugation and permutation of the external legs as follows

$$\mathcal{A}_{+-+}(p_1, p_2, p_3) = \mathcal{A}_{-++}(p_2, p_1, p_3), \quad (5.5)$$

$$\mathcal{A}_{+--}(p_1, p_2, p_3) = [\mathcal{A}_{-++}(p_1, p_2, p_3)]^*, \quad (5.6)$$

$$\mathcal{A}_{-+-}(p_1, p_2, p_3) = [\mathcal{A}_{-++}(p_2, p_1, p_3)]^*. \quad (5.7)$$

Note that complex conjugation must be performed only on the spinor-helicity structures and not on the helicity coefficient Ω_{-++} . We express the helicity coefficient in terms of form factors and find

$$\Omega_{-++} = s m_h^2 F_1. \quad (5.8)$$

When expanding the UV-renormalized helicity coefficient Ω_{-++} in the strong coupling constant, it is convenient to factor out the overall coefficient m_b^2/v . We obtain

$$\Omega_{-++} = \frac{m_b^2}{v} \sqrt{\frac{\alpha_s^3}{\pi}} \left[\Omega_{-++}^{(1l)} + \frac{\alpha_s}{2\pi} \Omega_{-++}^{(2l)} + \mathcal{O}(\alpha_s^2) \right]. \quad (5.9)$$

The ultraviolet renormalization and subtraction of infrared singularities described in the context of form factors, can be applied verbatim to the helicity coefficient Ω . Following the discussion in the previous Section, we write

$$\Omega_{-++}^{(2l)} = I_1(\epsilon) \Omega_{-++}^{(1l)} + \Omega_{-++}^{(2l),\text{fin}}, \quad (5.10)$$

where the operator $I_1(\epsilon)$ is defined in Eq.(4.7).

We renormalize the coupling constant at the scale $\mu = m_h$ in a theory with N_f active flavors. Since we are interested in the kinematic region where all scales are much larger than the bottom quark mass m_b , it is reasonable to perform a scheme change and define the amplitude in terms of the strong coupling constant which evolves with $N_f + 1$ active flavors. At the scale $\mu = m_h$, the relation is very simple and reads

$$\alpha_s^{(N_f)} = \alpha_s^{(N_f+1)} \left[1 - \frac{\alpha_s^{(N_f+1)}}{6\pi} \log \left(\frac{m_h^2}{m_b^2} \right) + \mathcal{O}(\alpha_s^2) \right]. \quad (5.11)$$

Eq.(5.11) implies the following relations for Catani's finite remainder of the helicity amplitude

$$\overline{\Omega}_{-++}^{(1l),\text{fin}} = \Omega_{-++}^{(1l),\text{fin}}, \quad \overline{\Omega}_{-++}^{(2l),\text{fin}} = \Omega_{-++}^{(2l),\text{fin}} - \frac{1}{2} \log \left(\frac{m_h^2}{m_b^2} \right) \overline{\Omega}_{-++}^{(1l),\text{fin}}, \quad (5.12)$$

where $\overline{\Omega}$ are the helicity coefficients corresponding to $\alpha_s^{(N_f+1)}$ evolved with $N_f + 1$ active flavors. We provide Catani's finite remainder of the helicity amplitudes defined in the scheme of Eq.(5.12) together with the arXiv submission of this paper.

6 Analytic continuation

We are interested in computing the two-loop contributions to scattering amplitudes for Higgs production processes at the LHC. The calculation of the decay amplitudes $H \rightarrow q\bar{q}g$ reported in the previous sections allows us to compute the scattering amplitudes for the three partonic processes $q\bar{q} \rightarrow Hg$, $qg \rightarrow Hq$ and $\bar{q}g \rightarrow H\bar{q}$, by crossing different particles from final to initial states and performing the relevant analytic continuation.

To describe the analytic continuation, we follow the notation introduced in Ref. [39]. To account for all helicity amplitudes of the two scattering processes $q\bar{q} \rightarrow Hg$ and $qg \rightarrow Hq$, we need to consider three kinematic regions that we will refer to as $(2a)_+$, $(3a)_+$ and $(4a)_+$, while the kinematic region of the decay process is referred to as $(1a)_+$. The regions are defined as

$$\text{region}(1a)_+ : \quad H(p_4) \rightarrow q(p_1) + \bar{q}(p_2) + g(p_3), \quad (6.1)$$

$$\text{region}(2a)_+ : \quad q(p_2) + \bar{q}(p_1) \rightarrow H(p_4) + g(p_3), \quad (6.2)$$

$$\text{region}(3a)_+ : \quad q(p_1) + g(p_3) \rightarrow H(p_4) + q(p_2), \quad (6.3)$$

$$\text{region}(4a)_+ : \quad q(p_2) + g(p_3) \rightarrow H(p_4) + q(p_1). \quad (6.4)$$

Note that, in contrast to $gg \rightarrow Hg$ and $q\bar{q} \rightarrow Hg$, for the process $qg \rightarrow Hq$ the region $(3a)_+$ is needed in order to obtain the helicity amplitudes with the opposite helicity assignment for the quarks from Ω_{-++} only.

The analytic continuation from region $(1a)_+$ to the other regions is described in detail in [39]. In particular, the spinor products in Eq.(5.4) are unchanged while the Goncharov polylogarithms appearing in the coefficient Ω_{-++} develop imaginary parts when computed in the different regions $(2a)_+$, $(3a)_+$ and $(4a)_+$. The imaginary parts can be extracted explicitly in terms of real valued functions following the strategy outlined in [39] using suitable changes of variables. Once the imaginary part is extracted, the numerical evaluation of Ω_{-++} can be performed using routines presented in [40, 41].

The analytic continuation is best understood by starting with the Euclidean non-physical region $(1a)_-$ and defined by

$$(1a)_- : \quad m_h^2, s, t, u < 0. \quad (6.5)$$

In the three ‘‘scattering regions’’ the Mandelstam invariants become

$$(2a)_+ : \quad m_h^2 > 0, \quad s > 0, \quad t, u < 0, \quad (6.6)$$

$$(3a)_+ : \quad m_h^2 > 0, \quad t > 0, \quad s, u < 0, \quad (6.7)$$

$$(4a)_+ : \quad m_h^2 > 0, \quad u > 0, \quad s, t < 0. \quad (6.8)$$

Continuation from region $(1a)_-$ to $(2a)_+$, $(3a)_+$ or $(4a)_+$, is achieved by providing an infinitesimal positive imaginary part to the following invariants

$$(2a)_+ : \quad m_h^2 \rightarrow m_h^2 + i0, \quad s \rightarrow s + i0, \quad (6.9)$$

$$(3a)_+ : \quad m_h^2 \rightarrow m_h^2 + i0, \quad t \rightarrow t + i0, \quad (6.10)$$

$$(4a)_+ : \quad m_h^2 \rightarrow m_h^2 + i0, \quad u \rightarrow u + i0. \quad (6.11)$$

For the three “scattering regions”, we define the new variables u_j and v_j as

$$(2a)_+ : \quad u_{2a} = -\frac{t}{s} = -\frac{y}{1-y-z}, \quad v_{2a} = \frac{m_h^2}{s} = \frac{1}{1-y-z}, \quad (6.12)$$

$$(3a)_+ : \quad u_{3a} = -\frac{u}{t} = -\frac{z}{y}, \quad v_{3a} = \frac{m_h^2}{t} = \frac{1}{y}, \quad (6.13)$$

$$(4a)_+ : \quad u_{4a} = -\frac{t}{u} = -\frac{y}{z}, \quad v_{4a} = \frac{m_h^2}{u} = \frac{1}{z}. \quad (6.14)$$

These variables satisfy the following constraints

$$0 \leq u_j \leq v_j, \quad 0 \leq v_j \leq 1 \quad \text{for } j = 2a, 3a, 4a. \quad (6.15)$$

In each region the extraction of the imaginary parts in terms of explicitly real-valued functions is achieved by changing variables in the Goncharov polylogarithms from (y, z) to (u_j, v_j) with $j = 2a, 3a, 4a$. As the result, the helicity amplitudes can be written as linear combinations of real-valued Goncharov polylogarithms of arguments (u_j, v_j) . We provide the one- and two-loop helicity coefficient Ω_{-++} in all regions described above together with the arXiv submission of this paper.

7 Collinear limit

In the kinematic limit of forward scattering the helicity amplitudes simplify. To derive the approximation for the amplitude, we start by considering the amplitude $H \rightarrow q\bar{q}g$ in the limit where quark and antiquark are emitted collinearly. By crossing the anti-quark and the gluon to the initial state, we then obtain the scattering amplitude for the partonic process $qg \rightarrow Hq$ in the collinear approximation.

More precisely, for the decay amplitude, we are interested in the situation $m_b^2 \ll s \ll m_h^2 \sim t \sim u$, which implies $1 - y - z = x \rightarrow 0$ and $z \sim y = (1 - z) \sim \mathcal{O}(1)$. For simplicity we define the abbreviations

$$L = \log(\kappa) = \log\left(\frac{-m_b^2}{m_h^2}\right) \quad \text{and} \quad \eta = \frac{\log(x/\kappa)}{\log(\kappa)}. \quad (7.1)$$

In the collinear limit $L \gg 1$ while $\eta \sim 1$. Expanding the helicity amplitude we find that at one loop all dependence on the other kinematical invariant drops and we are left with

$$\overline{\Omega}_{-++}^{(1),\text{fin}} = L^2 (\eta^2 - 1) - 4. \quad (7.2)$$

At two loops there is a residual functional dependence on y and the amplitudes are still too complicated to be reported here entirely.⁶ We write therefore the amplitude keeping the coefficients of the leading, next-to-leading and next-to-next-to-leading logarithms, which are relatively compact. We find

⁶Recall that in the limit $x \rightarrow 0$ we have $y \rightarrow 1 - z$.

$$\begin{aligned}
\bar{\Omega}_{-++}^{(2l),\text{fin}} &= i\pi\frac{3}{2}\bar{\beta}_0\bar{\Omega}_{-++}^{(1l),\text{fin}} + L^4\frac{5}{36}(1+\eta)^2(1-2\eta+3\eta^2) \\
&+ L^3(1+\eta)\left[(\eta^2-1)\left(\frac{3}{2}\log(y)+\frac{3}{2}\log(1-y)+\bar{\beta}_0\right)-\frac{1}{12}(3+\eta)(11\eta-15)\right] \\
&+ L^2\left\{(\eta^2-1)\left[\frac{29}{24}(\log(y)+\log(1-y))+\frac{3}{2}(\text{Li}_2(y)+\text{Li}_2(1-y))\right.\right. \\
&\left.\left.+\bar{\beta}_0\left(\frac{1}{4}(\log(y)+\log(1-y))-\frac{5}{3}\right)\right]+\frac{14\pi^2\eta^2}{9}-\frac{7\eta^2}{6}+\frac{10\pi^2\eta}{9}+\frac{\pi^2}{9}+\frac{7}{6}\right\}. \quad (7.3)
\end{aligned}$$

To obtain the scattering amplitude for the physical scattering process $qg \rightarrow qH$ (or similarly for $\bar{q}g \rightarrow \bar{q}H$) in the limit of a small momentum transfer from the quark line to the gluon-Higgs line one can of course use the general change of variables defined in Eqs.(6.13, 6.14). Nevertheless, in this limit we have to deal with much simpler functions of one variable only (in general, harmonic polylogarithms) and it is simpler to replace $y \rightarrow -\tilde{y} + i0$ and $m_h^2 \rightarrow m_h^2 + i0$ directly in Eq.(7.3). The sign of the imaginary part to be associated to y is determined noticing that in the scattering region $m_h^2 > 0$ and $t = -\tilde{t} < 0$ and therefore

$$y \rightarrow -\frac{(-t)}{m_h^2 + i0} = -\frac{\tilde{t}}{m_h^2} + i0 = -\tilde{y} + i0. \quad (7.4)$$

8 Conclusions

We described the calculation of the two-loop contribution to the scattering amplitude of the process $H \rightarrow q\bar{q}g$ mediated by a massive quark loop, in the kinematic limit where the quark mass is the smallest parameter in the process. For a typical hard LHC collision, this kinematic limit is expected to describe very well the contribution of loops of bottom quarks. The results presented in this paper provide the last missing ingredient required to obtain all the two-loop scattering amplitudes for the NLO QCD corrections to the top-bottom interference in Higgs plus jet production at the LHC.

In addition to their potential phenomenological relevance, these results are also interesting as a step towards understanding the structure of large logarithmic corrections that appear in amplitudes with virtual quarks loops that require a helicity flip. Resummation of these logarithms is not understood, and the results presented in this paper may help in further studies of this problem.

Acknowledgements

We would like to thank T. Hahn for his help with FormCalc. The research of K.M. was supported by the German Federal Ministry for Education & Research (BMBF) under grant O5H15VKCCA.

References

- [1] C. Anastasiou, C. Duhr, F. Dulat, E. Furlan, T. Gehrmann, F. Herzog, A. Lazopoulos, and B. Mistlberger, *High precision determination of the gluon fusion Higgs boson cross-section at the LHC*, *JHEP* **05** (2016) 058, [[arXiv:1602.00695](#)].
- [2] R. Boughezal, F. Caola, K. Melnikov, F. Petriello, and M. Schulze, *Higgs boson production in association with a jet at next-to-next-to-leading order in perturbative QCD*, *JHEP* **06** (2013) 072, [[arXiv:1302.6216](#)].
- [3] X. Chen, T. Gehrmann, E. W. N. Glover, and M. Jaquier, *Precise QCD predictions for the production of Higgs + jet final states*, *Phys. Lett.* **B740** (2015) 147–150, [[arXiv:1408.5325](#)].
- [4] R. Boughezal, F. Caola, K. Melnikov, F. Petriello, and M. Schulze, *Higgs boson production in association with a jet at next-to-next-to-leading order*, *Phys. Rev. Lett.* **115** (2015), no. 8 082003, [[arXiv:1504.07922](#)].
- [5] R. Boughezal, C. Focke, W. Giele, X. Liu, and F. Petriello, *Higgs boson production in association with a jet at NNLO using jetiness subtraction*, *Phys. Lett.* **B748** (2015) 5–8, [[arXiv:1505.03893](#)].
- [6] C. Arnesen, I. Z. Rothstein, and J. Zupan, *Smoking Guns for On-Shell New Physics at the LHC*, *Phys. Rev. Lett.* **103** (2009) 151801, [[arXiv:0809.1429](#)].
- [7] R. V. Harlander and T. Neumann, *Probing the nature of the Higgs-gluon coupling*, *Phys. Rev.* **D88** (2013) 074015, [[arXiv:1308.2225](#)].
- [8] A. Azatov and A. Paul, *Probing Higgs couplings with high p_T Higgs production*, *JHEP* **01** (2014) 014, [[arXiv:1309.5273](#)].
- [9] C. Grojean, E. Salvioni, M. Schlaffer, and A. Weiler, *Very boosted Higgs in gluon fusion*, *JHEP* **05** (2014) 022, [[arXiv:1312.3317](#)].
- [10] A. Banfi, A. Martin, and V. Sanz, *Probing top-partners in Higgs+jets*, *JHEP* **08** (2014) 053, [[arXiv:1308.4771](#)].
- [11] T. Neumann and C. Williams, *The Higgs boson at high p_T* , *Phys. Rev.* **D95** (2017), no. 1 014004, [[arXiv:1609.00367](#)].
- [12] H. Mantler and M. Wiesemann, *Top- and bottom-mass effects in hadronic Higgs production at small transverse momenta through LO+NLL*, *Eur. Phys. J.* **C73** (2013), no. 6 2467, [[arXiv:1210.8263](#)].
- [13] M. Grazzini and H. Sargsyan, *Heavy-quark mass effects in Higgs boson production at the LHC*, *JHEP* **09** (2013) 129, [[arXiv:1306.4581](#)].
- [14] A. Banfi, P. F. Monni, and G. Zanderighi, *Quark masses in Higgs production with a jet veto*, *JHEP* **01** (2014) 097, [[arXiv:1308.4634](#)].

- [15] E. Bagnaschi, R. V. Harlander, H. Mantler, A. Vicini, and M. Wiesemann, *Resummation ambiguities in the Higgs transverse-momentum spectrum in the Standard Model and beyond*, *JHEP* **01** (2016) 090, [[arXiv:1510.08850](#)].
- [16] K. Melnikov and A. Penin, *On the light quark mass effects in Higgs boson production in gluon fusion*, *JHEP* **05** (2016) 172, [[arXiv:1602.09020](#)].
- [17] F. Caola, S. Forte, S. Marzani, C. Muselli, and G. Vita, *The Higgs transverse momentum spectrum with finite quark masses beyond leading order*, *JHEP* **08** (2016) 150, [[arXiv:1606.04100](#)].
- [18] K. Melnikov, L. Tancredi, and C. Wever, *Two-loop $gg \rightarrow Hg$ amplitude mediated by a nearly massless quark*, *JHEP* **11** (2016) 104, [[arXiv:1610.03747](#)].
- [19] R. Mueller and D. G. Öztürk, *On the computation of finite bottom-quark mass effects in Higgs boson production*, *JHEP* **08** (2016) 055, [[arXiv:1512.08570](#)].
- [20] R. Bonciani, V. Del Duca, H. Frellesvig, J. M. Henn, F. Moriello, and V. A. Smirnov, *Two-loop planar master integrals for $Higgs \rightarrow 3$ partons with full heavy-quark mass dependence*, *JHEP* **12** (2016) 096, [[arXiv:1609.06685](#)].
- [21] R. K. Ellis, I. Hinchliffe, M. Soldate, and J. J. van der Bij, *Higgs Decay to $\tau^+ \tau^-$: A Possible Signature of Intermediate Mass Higgs Bosons at the SSC*, *Nucl. Phys.* **B297** (1988) 221–243.
- [22] U. Baur and E. W. N. Glover, *Higgs Boson Production at Large Transverse Momentum in Hadronic Collisions*, *Nucl. Phys.* **B339** (1990) 38–66.
- [23] P. Nogueira, *Automatic Feynman graph generation*, *J.Comput.Phys.* **105** (1993) 279–289.
- [24] T. Hahn, *Generating Feynman diagrams and amplitudes with FeynArts 3*, *Comput. Phys. Commun.* **140** (2001) 418–431, [[hep-ph/0012260](#)].
- [25] T. Gehrmann, M. Jaquier, E. Glover, and A. Koukoutsakis, *Two-Loop QCD Corrections to the Helicity Amplitudes for $H \rightarrow 3$ partons*, *JHEP* **1202** (2012) 056, [[arXiv:1112.3554](#)].
- [26] J. Vermaseren, *New features of FORM*, [math-ph/0010025](#).
- [27] T. Hahn and M. Perez-Victoria, *Automatized one loop calculations in four-dimensions and D-dimensions*, *Comput. Phys. Commun.* **118** (1999) 153–165, [[hep-ph/9807565](#)].
- [28] F. Tkachov, *A Theorem on Analytical Calculability of Four Loop Renormalization Group Functions*, *Phys.Lett.* **B100** (1981) 65–68.
- [29] K. Chetyrkin and F. Tkachov, *Integration by Parts: The Algorithm to Calculate beta Functions in 4 Loops*, *Nucl.Phys.* **B192** (1981) 159–204.

- [30] A. Smirnov, *Algorithm FIRE – Feynman Integral REduction*, *JHEP* **0810** (2008) 107, [[arXiv:0807.3243](#)].
- [31] A. V. Smirnov, *FIRE5: a C++ implementation of Feynman Integral REduction*, *Comput. Phys. Commun.* **189** (2015) 182–191, [[arXiv:1408.2372](#)].
- [32] C. W. Bauer, A. Frink, and R. Kreckel, *Introduction to the GiNaC framework for symbolic computation within the C++ programming language*, *J.Symb.Comput.* **33** (2002) 1–12, [[cs/0004015](#)].
- [33] C. Studerus, *Reduze-Feynman Integral Reduction in C++*, *Comput.Phys.Commun.* **181** (2010) 1293–1300, [[arXiv:0912.2546](#)].
- [34] A. von Manteuffel and C. Studerus, *Reduze 2 - Distributed Feynman Integral Reduction*, [arXiv:1201.4330](#).
- [35] R. Lewis, *Computer Algebra System Fermat*. <http://home.bway.net/lewis/>.
- [36] T. Gehrmann and E. Remiddi, *Two loop master integrals for $\gamma^* \rightarrow 3$ jets: The Planar topologies*, *Nucl.Phys.* **B601** (2001) 248–286, [[hep-ph/0008287](#)].
- [37] S. Catani, *The Singular behavior of QCD amplitudes at two loop order*, *Phys.Lett.* **B427** (1998) 161–171, [[hep-ph/9802439](#)].
- [38] L. J. Dixon, *Calculating scattering amplitudes efficiently, in QCD and beyond. Proceedings, Theoretical Advanced Study Institute in Elementary Particle Physics, TASI-95, Boulder, USA, June 4-30, 1995*, pp. 539–584, 1996. [hep-ph/9601359](#).
- [39] T. Gehrmann and E. Remiddi, *Analytic continuation of massless two loop four point functions*, *Nucl.Phys.* **B640** (2002) 379–411, [[hep-ph/0207020](#)].
- [40] T. Gehrmann and E. Remiddi, *Numerical evaluation of harmonic polylogarithms*, *Comput.Phys.Commun.* **141** (2001) 296–312, [[hep-ph/0107173](#)].
- [41] T. Gehrmann and E. Remiddi, *Numerical evaluation of two-dimensional harmonic polylogarithms*, *Comput.Phys.Commun.* **144** (2002) 200–223, [[hep-ph/0111255](#)].